Preprints.org

Article

Not peer-reviewed version

Preparation and Characterization of a Curcumin Solid Dispersion with Enhanced Solubility and Hepato-protective Efficacy Against Non-Alcoholic Fatty Liver Disease

Xiaodong Gong , Qinghua Zang , Huaijie Jin , Jiuba Zhang , Yu Li , Lianlin Su , Wenhong Zhu , Zhijun Guo , Mingxuan Li , Chunqin Mao , Changcan Shi * , Tulin Lu *

Posted Date: 26 October 2026

Keywords: curcumin; amorphous solid dispersion; polyvinylpyrrolidone K30; phosphatidylcholine; solubility; dissolution; bioavailability; non-alcoholic fatty liver disease

Preprints.org is a free multidisciplinary platform providing preprint service that is dedicated to making early versions of research outputs permanently available and citable. Preprints posted at Preprints.org appear in Web of Science, Crossref, Google Scholar, Scilit, Europe PMC, OpenAlex.

Copyright: This open access article is published under a Creative Commons CC BY 4.0 license, which permit the free download, distribution, and reuse, provided that the author and preprint are cited in any reuse.

Preprints.org | NOT PEER-REVIEWED | Posted: 26 October 2026 https://doi.org/10.20944/preprints202610.2537.v1

Disclaimer/Publisher's Note: The statements, opinions, and data contained in all publications are solely those of the individual author(s) and contributor(s) and not of MDPI and/or the editor(s). MDPI and/or the editor(s) disclaim responsibility for any injury to people or property resulting from any ideas, methods, instructions, or products referred to in the content.

Article

Preparation and Characterization of a Curcumin Solid Dispersion with Enhanced Solubility and Hepatoprotective Efficacy Against Non-Alcoholic Fatty Liver Disease

Xiaodong Gong, Qinghua Zang, Huaijie Jin, Jiuba Zhang, Yu Li, Lianlin Su, Wenhong Zhu, Zhijun Guo, Mingxuan Li, Chunqin Mao, Changcan Shi * and Tulin Lu *

College of Pharmacy, Nanjing University of Chinese Medicine, Nanjing 210023, China

* Correspondence: cshi@njucm.edu.cn (C.S.); ltl2021@njucm.edu.cn (T.L.)

Abstract

Background/Objectives: Curcumin has potential hepatoprotective effects in non-alcoholic fatty liver disease (NAFLD), but its poor aqueous solubility limits formulation development. This study aimed to prepare a curcumin solid dispersion (CSD) using polyvinylpyrrolidone K30 (PVP K30) and phosphatidylcholine to evaluate its physicochemical properties and hepatoprotective effects. **Methods:** CSD was prepared by solvent evaporation at a curcumin/phosphatidylcholine/PVP K30 weight ratio of 1:2:3. X-ray diffraction, differential scanning calorimetry, Fourier-transform infrared spectroscopy, and scanning electron microscopy were used for characterization. Apparent solubility and in vitro dissolution were assessed in buffers at pH 1.2, 4.5, and 6.8. Raw curcumin and a corresponding physical mixture were used as comparators. Hepatoprotective effects were investigated in a high-fat diet/lipopolysaccharide-induced experimental NAFLD model using serum biochemical markers, hepatic inflammatory cytokines, and liver histology. The animal study compared oral CSD at curcumin-equivalent doses of 50 and 100 mg/kg/day with unformulated curcumin at 200 mg/kg/day. **Results:** The dispersion showed diffraction and thermal profiles consistent with amorphization of curcumin. Apparent solubility reached 184.2, 232.6, and 292.1 μg/mL at pH 1.2, 4.5, and 6.8, respectively. At pH 1.2, the reported 90 min cumulative dissolution increased from 8.8% for unformulated curcumin to 87.9% for CSD. CSD treatment was associated with lower serum ALT and ALP levels, reduced hepatic lipid accumulation, and decreased hepatic TNF-α, IL-6, and IL-1β levels. **Conclusions:** The PVP K30/phosphatidylcholine-based solid dispersion improved curcumin's apparent solubility and dissolution and showed hepatoprotective effects in an experimental NAFLD model. These findings support further evaluation of this formulation approach.

Keywords: curcumin; amorphous solid dispersion; polyvinylpyrrolidone K30; phosphatidylcholine; solubility; dissolution; bioavailability; non-alcoholic fatty liver disease

1. Introduction

Non-alcoholic fatty liver disease (NAFLD) is the most prevalent chronic liver disease worldwide, with a global prevalence of 32.4% and rates exceeding 60% in individuals with obesity or type 2 diabetes [1]. Its disease spectrum ranges from simple steatosis to metabolic dysfunction-associated steatohepatitis (MASH), which is histologically characterized by hepatocellular ballooning, lobular inflammation, and fibrosis, and can progress to cirrhosis and hepatocellular carcinoma. Currently, effective pharmacotherapies are severely lacking and standard management relies predominantly on lifestyle modifications, which suffer from poor long-term adherence and variable efficacy [2]. Thus, there remains a substantial unmet medical need in NAFLD treatment.

© 2026 by the author(s). Distributed under a Creative Commons CC BY license.

Preprints.org | NOT PEER-REVIEWED | Posted: 26 October 2026 https://doi.org/10.20944/preprints202610.2537.v1

Curcumin, a lipophilic polyphenolic compound isolated from the rhizome of *Curcuma longa* (turmeric), has drawn substantial research attention as a promising natural agent for managing metabolic and inflammatory disorders including NAFLD [3]. This phytochemical exhibits a wide range of pharmacological activities, most prominent of which are antioxidant, anti-inflammatory, and lipid-regulating effects [4,5]. A large body of preclinical evidence has confirmed that curcumin supplementation alleviates hepatic lipid accumulation, decreases serum alanine aminotransferase (ALT) and aspartate aminotransferase (AST) levels, and reduces circulating triglyceride and total cholesterol concentrations in multiple diet-induced and chemically induced NAFLD models [6]. The mechanisms underlying the hepatoprotective effects of curcumin are multifactorial. Curcumin enhances the endogenous antioxidant defense system by upregulating nuclear factor erythroid 2-related factor 2 (Nrf2) and its downstream detoxifying enzymes, thereby reducing oxidative stress [7]. Meanwhile, curcumin inhibits the production of pro-inflammatory cytokines by suppressing the nuclear factor-kappa B (NF-κB) signaling pathway [8], and regulates lipid homeostasis by activating AMPK and downregulating lipogenic transcription factors such as SREBP-1c [9]. Furthermore, curcumin improves insulin sensitivity, which indirectly ameliorates the metabolic environment that promotes hepatic steatosis [10].

Despite its diverse pharmacological activities, the clinical translation of curcumin is severely hampered by its extremely low oral bioavailability. This limitation arises from poor aqueous solubility, insufficient intestinal permeability, and extensive first-pass metabolism, which ultimately lead to plasma and hepatic concentrations that are well below the therapeutic threshold [11,12]. To overcome this challenge, a variety of drug delivery systems including inclusion complexes, micelles, liposomes, and nanoparticles have been developed to improve the solubility, stability, and absorption of curcumin. Among these formulation strategies, solid dispersions have been extensively explored for curcumin delivery [13–15]. Prior work has utilized carriers such as PVP K30/HPMC binary systems and self-micellizing formulations to improve curcumin dissolution and pharmacokinetic profiles in rats [16], and several studies have incorporated piperine to inhibit curcumin metabolism [17–19]. However, most existing studies have focused exclusively on formulation development alone, or on the pharmacological evaluation of unformulated curcumin in NAFLD models. This creates a critical research gap: no integrated investigation has yet established the connection between formulation-improved solubility and in vivo therapeutic efficacy of curcumin for NAFLD. This unaddressed gap provides the core rationale for the present study.

The present study aimed to develop and systematically evaluate a curcumin solid dispersion for the treatment of NAFLD. Specifically, we fabricated the solid dispersion using PVP K30 and phosphatidylcholine (PC) as hydrophilic carriers via the solvent evaporation method. Comprehensive physicochemical characterization of the prepared formulation was conducted, including solubility determination, X-ray diffraction (XRD), differential scanning calorimetry (DSC), scanning electron microscopy (SEM), Fourier-transform infrared spectroscopy (FTIR), and in vitro dissolution testing, to confirm the successful conversion of crystalline curcumin to an amorphous state and evaluate its improved release profile. Subsequently, the hepatoprotective efficacy of curcumin solid dispersion was assessed in a high-fat diet (HFD)-induced NAFLD mouse model, with particular focus on the dose-dependent effects on serum biochemical parameters and inflammatory responses. Through the integration of formulation development and in vivo pharmacodynamic evaluation, this study provides a robust preclinical foundation for advancing curcumin solid dispersion as a potential therapeutic strategy for NAFLD.

2. Materials and Methods

2.1. Materials

Curcumin raw material (purity ≥ 98%) was purchased from Adamas-beta (Shanghai, China). Polyvinylpyrrolidone K30 (PVP K30, average molecular weight 44,000–54,000, K-value ≈ 30) was obtained from BASF (Shanghai, China). Phosphatidylcholine was purchased from Adamas-beta

© 2026 by the author(s). Distributed under a Creative Commons CC BY license.

Preprints.org | NOT PEER-REVIEWED | Posted: 26 October 2026 https://doi.org/10.20944/preprints202610.2537.v1

(Shanghai, China). Lipopolysaccharide (LPS, *Escherichia coli* O55:B5) was purchased from Yuanye Biotechnology (Shanghai, China). Commercial assay kits for measuring serum alanine aminotransferase (ALT), alkaline phosphatase (ALP), total cholesterol (TC), high-density lipoprotein cholesterol (HDL-C), and low-density lipoprotein cholesterol (LDL-C) were obtained from Qiangsheng Biology (Zhejiang, China). ELISA kits for quantifying tumor necrosis factor-alpha (TNF-α), interleukin-6 (IL-6), and interleukin-1β (IL-1β) were procured from Hangzhou Fuyou Biotechnology (Zhejiang, China). All other chemicals and solvents used were of the highest purity grade commercially available.

2.2. Preparation of Curcumin Solid Dispersion (CSD)

Solid dispersions were prepared via the solvent evaporation method, using phosphatidylcholine (PC) as the surfactant and PVP K30 as the hydrophilic carrier, with a curcumin-to-PC-to-PVP K30 weight ratio of 1:2:3. Briefly, accurately weighed curcumin (6 g), PC (12 g), and PVP K30 (18 g) were fully dissolved in 120 mL of a mixed solvent of anhydrous ethanol and tetrahydrofuran（volume ratio 1:1）under continuous magnetic stirring at 300 rpm, until a clear homogeneous solution was obtained. The solution was then subjected to solvent removal via rotary evaporation under reduced pressure at a water bath temperature of 40°C with a rotation speed of 60 rpm, until all solvent was completely evaporated. The obtained solid residue was further dried in a vacuum oven at 70°C for 72 hours to ensure complete removal of residual solvent. The dried product was gently ground in an agate mortar and passed through a 50-mesh sieve to obtain a fine powder with uniform particle size. The final curcumin solid dispersion (CSD) powder was stored at 4°C in the dark prior to subsequent characterization and experiments. For comparison, a physical mixture (PM) of curcumin, PC, and PVP K30 at the same weight ratio was also prepared by simply blending the three components in a mortar for 10 minutes without solvent treatment or heating, and stored under identical conditions.

2.3. Characterization of Curcumin Solid Dispersion

2.3.1. Solubility Determination

The apparent solubility of curcumin, physical mixture (PM), and the prepared curcumin solid dispersion (CSD) was determined using the shake-flask method. Briefly, aliquots of curcumin, PM, and CSD, each containing 10 mg of curcumin (at the pre-specified carrier ratios), were added to 5 mL of pH 1.2, 4.5, and 6.8 buffer solutions in separate sealed glass vials. All vials were incubated in a constant-temperature water bath shaker and agitated at 100 rpm and 37°C for 24 hours until equilibrium was reached. Subsequently, aliquots of the equilibrated suspension were withdrawn and immediately filtered through a 0.45 μm PTFE syringe filter. Chromatographic separation was performed on an Xterra C18 column (4.6 × 50 mm, 5 μm; Waters) maintained at a constant temperature of 35°C. The mobile phase consisted of 0.05% formic acid in ultrapure water (solvent A) and acetonitrile (solvent B), with isocratic elution at a constant proportion of 40% solvent B. The flow rate was set to 1.0 mL/min with a total run time of 7 minutes, and the eluate was monitored at a wavelength of 230 nm. All samples were analyzed in triplicate.

2.3.2. X-Ray Diffraction (XRD)

X-ray diffraction patterns of curcumin, PC, PVP K30, physical mixture (PM), and the prepared curcumin dried powder (CSD) were collected using an X-ray diffractometer (Mini Flex 600, Rigaku) to characterize the crystalline status of curcumin in the formulation. All samples were scanned over a 2θ range of 3° to 40°, with a scanning rate of 2°/min and a step size of 0.02°. Measurements were performed using Cu-Kα radiation (λ = 1.5406 Å) at an operating voltage of 40 kV and an operating current of 15 mA.

© 2026 by the author(s). Distributed under a Creative Commons CC BY license.

Preprints.org | NOT PEER-REVIEWED | Posted: 26 October 2026 https://doi.org/10.20944/preprints202610.2537.v1

2.3.3. Differential Scanning Calorimetry (DSC)

Thermal analysis was conducted via differential scanning calorimetry (Q20, TA Instruments) to characterize drug-carrier interactions and the physical state of curcumin in the prepared solid dispersions. Accurately weighed 20 mg aliquots of curcumin, PC, PVP K30, physical mixture (PM), and curcumin solid dispersion (CSD) were sealed in aluminum pans with pinhole lids, and an empty sealed aluminum pan was used as the reference. All samples were heated from 25°C to 200°C at a constant heating rate of 10°C/min under a nitrogen atmosphere with a flow rate of 50 mL/min.

2.3.4. Scanning Electron Microscopy (SEM)

The surface morphology of curcumin and CSD was characterized via scanning electron microscopy (model IEM-30, manufactured by COXEM). Specifically, the powdered samples were mounted onto double-sided carbon conductive tape, which was fixed on aluminum stubs. The samples were then sputter-coated with gold under vacuum for 60 seconds to improve electrical conductivity. Subsequently, the samples were imaged at an accelerating voltage of 10 kV with a working distance of 100 μm to characterize the surface topography and particle morphology.

2.3.5. Fourier-Transform Infrared Spectroscopy (FTIR)

FTIR spectroscopy was performed on a Cary 630 Fourier-transform infrared spectrometer (Agilent Technologies) to characterize the molecular-level interactions between curcumin and the carrier material in the prepared solid dispersion. Approximately 20 mg samples of pure curcumin, physical mixture (PM), and curcumin solid dispersion (CSD) were tested according with the instrument's operating specifications. Spectra were collected over the wavenumber range of 400–4000 cm^{-1} at a resolution of 4 cm^{-1}, with eight scans co-added per spectrum to enhance the signal-to-noise ratio.

2.3.6. In Vitro Dissolution Study

The in vitro dissolution profiles of curcumin, physical mixture (PM), and the prepared curcumin solid dispersion (CSD) were compared via a dissolution apparatus (FADT-1202RC, FOCS) in accordance with the United States Pharmacopeia (USP) paddle method (Apparatus II). Samples equivalent to 100 mg of curcumin were accurately weighed and transferred into dissolution vessels loaded with 900 mL of dissolution medium (pH 1.2 hydrochloric acid solution, pH 4.5 acetic acid buffer solution, pH 6.8 phosphate buffer solution), which was supplemented with 0.2% sodium dodecyl sulfate (SDS) to maintain sink conditions. The dissolution medium was kept at a constant temperature of 37.0 ± 0.5°C, and agitation was performed at a paddle rotation speed of 75 rpm. At pre-established time intervals (5, 15, 30, 45, 60 and 90 minutes), aliquots were withdrawn from the vessels, filtered through 10 μm syringe filters, and quantified via the validated HPLC method described in Section 2.3.1 above. The cumulative release percentage of curcumin was plotted as a function of time. The dissolution profiles of CSD were compared with those of curcumin and PM to evaluate the dissolution enhancement effect of solid dispersion on drug release. All experiments were performed in triplicate.

2.4. Pharmacodynamic Study

2.4.1. Animals and Dosing Protocol

Male C57BL/6 mice weighing 18–22 g (6–8 weeks, n = 30) were purchased from Jiangsu Qinglongshan Biotechnology Co., Ltd., China (certification of quality: SCXK (Su) 2024–0001）. All animals were housed under standard laboratory conditions: ambient temperature maintained at 25 ± 5 °C, 12 h light/dark cycle, with free access to standard rodent chow and purified water. All experimental procedures involving animals were approved by the Laboratory Animal Ethics Committee of Nanjing University of Chinese Medicine (approval No. A202312050024) on 5 December 2023. After one week of adaptive feeding, the mice were randomly divided into five groups (n = 6 per group), which adhered to the following regimens for 15 weeks: (1) normal control (normal chow + saline i.p. +

© 2026 by the author(s). Distributed under a Creative Commons CC BY license.

Preprints.org | NOT PEER-REVIEWED | Posted: 26 October 2026 https://doi.org/10.20944/preprints202610.2537.v1

vehicle); (2) HFD+LPS model (HFD + LPS i.p. + vehicle); (3) curcumin group (HFD + LPS + curcumin 200 mg·kg^{-1}·d^{-1} p.o.); and (4-5) curcumin formulation groups (HFD + LPS + formulation at curcumin-equivalent doses of 50, and 100 mg·kg^{-1}·d^{-1} p.o., respectively). Lipopolysaccharide (LPS) was administered intraperitoneally at 1 mg/kg twice weekly, starting from week 2 and continuing for 15 weeks. Vehicle and drug treatments were administered via oral gavage during weeks 9-15. The HFD was characterized by 60 % fat-derived calories. The animal body weight, serum biochemistry, liver histology, and hepatic inflammatory cytokine levels were measured to evaluate changes in the corresponding indicators among the groups.

Body weights of the mice were monitored weekly. At the 15th week, the mice were anesthetized with 1.0 g/kg urethane via intraperitoneal injection. Blood samples were collected from the retro-orbital plexus into additive-free plain tubes without anticoagulants, then allowed to clot at room temperature for 60 minutes. Subsequently, the samples were centrifuged at 4000×g for 3 minutes at 4°C, and the obtained serum supernatants were carefully aspirated and stored at -80°C until subsequent biochemical analysis. Mice were euthanized, followed by cervical dislocation as a confirmatory method of death, after which livers were harvested. The mouse livers were rapidly excised, rinsed thoroughly with ice-cold 0.9% (w/v) normal saline to remove residual blood and blotted dry. For histopathological evaluation, a portion of each liver specimen was immediately fixed in 4% paraformaldehyde solution at room temperature for no less than 24 hours to prepare for subsequent paraffin embedding. The remaining liver tissues were stored at -80°C for further biochemical analysis.

2.4.2. Biochemical and Inflammatory Marker Analysis

2.4.2.1. Serum Biochemical Parameters

Serum levels of alanine aminotransferase (ALT), alkaline phosphatase (ALP), and lipid profiles including total cholesterol (TC), high-density lipoprotein cholesterol (HDL-C) and low-density lipoprotein cholesterol (LDL-C) were quantified with commercial assay kits purchased from Qiangsheng Biology (Zhejiang, China), following the manufacturer's protocols. All measurements were conducted on a Beckman Coulter AU480 automatic biochemical analyzer at the corresponding specified wavelengths.

2.4.2.2. Inflammatory Cytokine Levels in Liver

The concentrations of pro-inflammatory cytokines, including TNF-α, IL-6, and IL-1β, were quantified in the supernatants of liver homogenates using enzyme-linked immunosorbent assay (ELISA) kits pre-validated for mouse samples according to the manufacturer's instructions. Briefly, samples and standard solutions were added to pre-coated microplates, incubated with biotinylated detection antibodies, and subsequently conjugated with streptavidin-horseradish peroxidase (HRP). Following the addition of the chromogenic substrate tetramethylbenzidine (TMB), the reaction was terminated with stop solution (acid), and the optical density (OD) was measured at a wavelength of 450 nm using a microplate reader. The concentration of each target cytokine in the test samples was calculated by interpolating the measured sample OD values against the generated standard curve.

2.4.2.3. Statistical Analysis for Biochemical Data

All biochemical data are presented as mean ± standard deviation (SD). One-way analysis of variance (ANOVA) was performed to assess the statistical significance of differences in the measured parameters among groups including the normal control group, model group, curcumin group and curcumin solid dispersion (CSD) group, followed by Dunnett's test for post-hoc multiple comparisons. A P value of < 0.05 was defined as the threshold for statistical significance.

© 2026 by the author(s). Distributed under a Creative Commons CC BY license.

Preprints.org | NOT PEER-REVIEWED | Posted: 26 October 2026 https://doi.org/10.20944/preprints202610.2537.v1

2.4.3. Histopathological Examination

2.4.3.1. Hematoxylin and Eosin (H&E) Staining

For hematoxylin and eosin (H&E) staining, paraffin sections were subjected to deparaffinization treatment. The sections were stained with hematoxylin for 3 minutes, rinsed, differentiated for 3-5 seconds, rinsed again, and stained blue in bluing solution for 3-6 seconds, followed by a final water wash. After dehydration with 95% ethanol, the sections were counterstained with eosin for 15 seconds. Subsequently, the sections were dehydrated sequentially in absolute ethanol and n-butanol, cleared in xylene, and mounted with neutral balsam. Finally, the stained sections were examined under a light microscope, and representative images were acquired for subsequent analysis.

2.4.3.2. Oil Red O Staining

For Oil Red O staining, frozen liver sections were fixed and stained with Oil Red O solution in the dark for 8-10 min. The sections were then differentiated with 60% isopropanol to remove non-specific background staining and rinsed thoroughly with distilled water. After counterstaining with hematoxylin and treatment with differentiation solution, a bluing solution was applied, and the sections were rinsed with water. Finally, the sections were mounted with glycerol gelatin and imaged under a light microscope.

3. Results

3.1. Preparation and Characterization of CSD

3.1.1. Solubility Determination

The equilibrium solubility of raw curcumin and CSD were determined in different pH solution at 37℃ via the shake-flask method, and the corresponding results are summarized in Table 1.

Table 1. Solubility of raw curcumin, PM, and CSD in different solutions (mean ± SD, n = 3).

Sample	Apparent Solubility (μg/mL)		
	pH 1.2	pH 4.5	pH 6.8
Curcumin	0±0	0±0	0±0
Physical mixture (PM)	0±0	11.1±0.35	15.4±0.97
curcumin solid dispersion （CSD）	184.2 ±20.4	232.6 ±50.1	292.1 ±18.5

As shown in Table 1, the equilibrium solubility of curcumin was undetectable across all tested solutions, confirming its practically insoluble property. Compared with pure curcumin, the physical mixture (PM) exhibited a slight increase in curcumin dissolution, which is attributed to the solubilization effect of micellization. In contrast to the physical mixture, the CSD sample showed a dramatic improvement in solubility, with solubility reaching 184.2 μg/mL, 232.6 μg/mL, and 292.1 μg/mL in the three tested solutions respectively. This significant solubility enhancement can be attributed to the amorphous transformation of curcumin and the formation of intermolecular hydrogen bonds between curcumin and the carrier.

3.1.2. X-Ray Diffraction (XRD)

The crystalline properties of curcumin, physical mixture (PM), and optimized curcumin solid dispersion (CSD) were characterized by X-ray diffraction (XRD, Figure 1A). Curcumin exhibited multiple intense and sharp characteristic diffraction peaks at 2θ values of 8.8°, 12.2°, 14.5°, 17.2°, 18.1°,

© 2026 by the author(s). Distributed under a Creative Commons CC BY license.

Preprints.org | NOT PEER-REVIEWED | Posted: 26 October 2026 https://doi.org/10.20944/preprints202610.2537.v1

21.1°, 23.3°, 24.7°, 25.7° and 27.4°, confirming its high crystallinity. A similar diffraction pattern for pure curcumin is found in previously published research [20]. Pure PC and PVP K30 presented broad diffuse halos without distinct diffraction peaks, indicating their amorphous nature. The diffraction pattern of PM was essentially a superposition of the characteristic peaks of crystalline curcumin and the diffuse halos of amorphous PC and PVP K30, with no significant shifts in peak positions or changes in peak intensities. In sharp contrast, all characteristic crystalline peaks of curcumin completely disappeared in the XRD pattern of the CSD, leaving only a broad amorphous halo consistent with that of the carrier matrix. This result confirms that curcumin was successfully converted from the crystalline state to the amorphous state in the PVP K30 matrix, which is the fundamental mechanism for the improved dissolution and bioavailability of the solid dispersion.

3.1.3. Differential Scanning Calorimetry (DSC)

DSC is an essential tool for detecting both the endothermic (melting) and exothermic transitions like crystallization [21]. The DSC thermograms of curcumin, PC, PVP K30, the physical mixture (PM) and the curcumin solid dispersion (CSD) were compared (Figure 1B). Curcumin presented a sharp endothermic melting peak at 183.48 °C, which confirms its crystalline nature. Neither PC nor PVP K30 exhibited distinct thermal events within the scanning temperature range of 25-200 °C. In the physical mixture, the melting peak of curcumin remained detectable but showed a slight reduction in intensity, verifying that curcumin maintained most of its crystallinity after simple physical mixing. Notably, this characteristic peak was completely absent in the CSD, proving that curcumin was converted to an amorphous or molecularly dispersed state in the PVP K30 matrix, which is beneficial for improving drug dissolution and bioavailability.

3.1.4. Scanning Electron Microscopy (SEM)

The surface morphology of curcumin and the CSD was characterized by SEM (Figure 1C). Curcumin presented irregular rod-shaped crystals consistent with its intrinsic crystalline property. In contrast, CSD existed as blocky or nearly spherical microparticles with a smooth surface, and the characteristic crystals of curcumin were no longer detected. This uniform morphology provides direct visual evidence confirming that curcumin was successfully incorporated into the PVP K30 carrier and dispersed at the molecular level.

3.1.5. Fourier-Transform Infrared Spectroscopy (FTIR)

The FT-IR spectra of curcumin, the physical mixture (PM) and the curcumin solid dispersion (CSD) were acquired (Figure 1D). The spectrum of curcumin presented distinct, well-resolved absorption peaks around 3500 cm^{-1} and within the fingerprint region (e.g., 1626, 1600, 1424, 1150 cm^{-1}), which are characteristic signals of its crystalline structure. The spectral profile of the PM was nearly identical to that of free curcumin, with only a minor reduction in absorption intensity. This observation confirms that simple physical mixing does not disrupt the crystalline lattice of curcumin. In contrast, the spectrum of CSD exhibited marked changes: the O-H stretching band was significantly broadened, and most sharp characteristic peaks in the fingerprint region were substantially attenuated or completely disappeared. Concurrently, the characteristic absorption bands of phosphatidylcholine were observed at 2922 cm^{-1} (assigned to C-H stretching) and 1737 cm^{-1} (assigned to C=O stretching), while the characteristic carbonyl absorption band of PVP K30 appeared at 1655 cm^{-1}. Similar spectral differences between crystalline and amorphous forms of phytochemicals have been documented in previous reports [22]. These observed peak shifts and broadening effects confirm the formation of intermolecular hydrogen bonds and other non-covalent interactions between curcumin, PVP K30 and phosphatidylcholine in the solid dispersion, accompanied by the phase transition of curcumin from a crystalline state to an amorphous state.

© 2026 by the author(s). Distributed under a Creative Commons CC BY license.

Preprints.org | NOT PEER-REVIEWED | Posted: 26 October 2026 https://doi.org/10.20944/preprints202610.2537.v1

3.1.6. In Vitro Dissolution Study

The dissolution profiles of curcumin, physical mixture (PM) and curcumin solid dispersion (CSD) were evaluated in three biorelevant media (pH 1.2, pH 4.5 and pH 6.8) to simulate the gastrointestinal tract environment (Figure 1E). Due to its inherent hydrophobicity and crystalline structure, curcumin showed extremely low cumulative release in all tested media, with only 8.8%, 23.5% and 5.4% of curcumin dissolved within 90 minutes. The PM group achieved a moderate improvement in dissolution performance, which can be attributed to the wetting effect of PVP K30. However, the dissolution release remained limited because curcumin still maintained its crystalline structure (e.g., 43.2% dissolution at 90 minutes in pH 1.2 medium). In contrast, CSD exhibited a significantly improved dissolution performance across all tested pH conditions. At pH 1.2, CSD released 87.9% of the loaded curcumin within 90 minutes, which is approximately 10-fold higher than that of raw curcumin. Similarly, in a pH 4.5 dissolution medium, the cumulative release of curcumin from CSD reached 101.3% at 90 minutes, corresponding to an approximately 4.3-fold improvement compared to raw curcumin; in pH 6.8 buffer, the cumulative release reached 101.4% at 90 minutes, representing an approximately 18.7-fold increase. The improvement in dissolution was observed throughout the entire release period, indicating that amorphous solid dispersion can effectively enhance the solubility and dissolution rate of curcumin regardless of the pH environment. The superior dissolution performance of CSD at pH 4.5 and pH 6.8 compared to pH 1.2 can be attributed to two factors: first, the pH-dependent solubility of curcumin, which increases as pH rises due to the partial deprotonation of its phenolic hydroxyl groups; second, the improved wettability and swelling capacity of the PVP K30 carrier in near-neutral media. The overall trend confirms that the CSD formulation can reliably overcome the poor aqueous solubility of curcumin. Complete results of the dissolution tests are summarized in Tables 2-4.

Table 2. Dissolution profiles of Curcumin, PM, and CSD at pH 1.2 buffer (mean ± SD, n = 3).

Name	Dissolution at pH 1.2 (%)					
	5 min	15 min	30 min	45 min	60 min	90 min
Curcumin	2.0±0.6	1.5±0.1	14.4±3.3	11.0±2.6	12.0±0.5	8.8±0.3
Physical mixture (PM)	0.7±0.7	2.0±1.2	21.2±5.6	27.9±6.1	35.1±4.5	43.2±1.0
Curcumin solid dispersion (CSD)	2.1±0.9	3.6±1.4	26.0±4.1	48.1±1.4	66.0±3.4	87.9±3.1

Table 3. Dissolution profiles of Curcumin, PM, and CSD at pH 4.5 buffer (mean ± SD, n = 3).

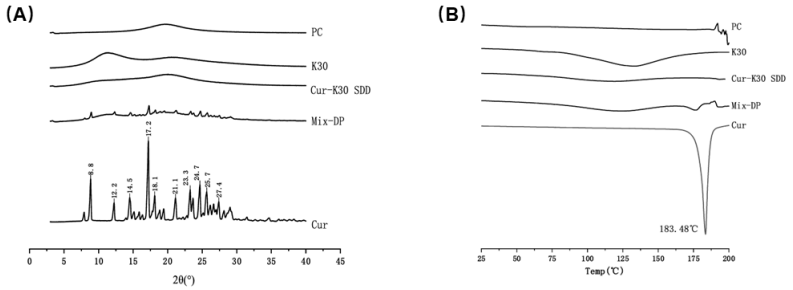
Name	Dissolution at pH 4.5 (%)					
	5 min	15 min	30 min	45 min	60 min	90 min
Curcumin	12.8±4.1	16.2±5.6	28.0±4.2	14.7±5.6	20.3±4.3	23.5±4.2
Physical mixture (PM)	20.3±10.5	28.6±6.3	35.3±4.9	32.4±5.4	38.1±3.9	42.5±0.9
Curcumin solid dispersion (CSD)	18.8±10.4	52.6±18.0	79.9±12.5	93.2±4.7	99.5±0.8	101.3±2.0

© 2026 by the author(s). Distributed under a Creative Commons CC BY license.

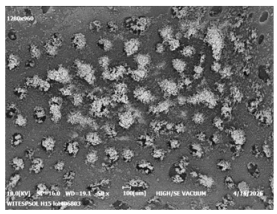
Preprints.org | NOT PEER-REVIEWED | Posted: 26 October 2026 https://doi.org/10.20944/preprints202610.2537.v1

Table 4. Dissolution profiles of Curcumin, PM, and CSD at pH 6.8 buffer (mean ± SD, n = 3).

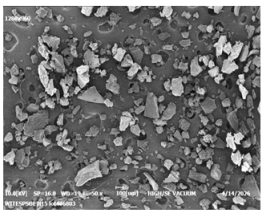
Name	Dissolution at pH 6.8 (%)					
	5 min	15 min	30 min	45 min	60 min	90 min
Curcumin	1.8±0.3	3.8±0.3	6.7±0.2	7.1±0.1	19.0±4.8	5.4±0.8
Physical mixture (PM)	4.9±0.9	11.2±2.2	19.0±3.8	25.0±6.4	29.6±5.3	40.3±4.1
Curcumin solid dispersion (CSD)	24.8±6.7	49.3±6.8	66.7±10.4	76.7±10.7	85.6±9.6	101.4±3.6



(C)



SEM of Curcumin (x50)



SEM of CSD (x50)

© 2026 by the author(s). Distributed under a Creative Commons CC BY license.

Preprints.org | NOT PEER-REVIEWED | Posted: 26 October 2026 https://doi.org/10.20944/preprints202610.2537.v1

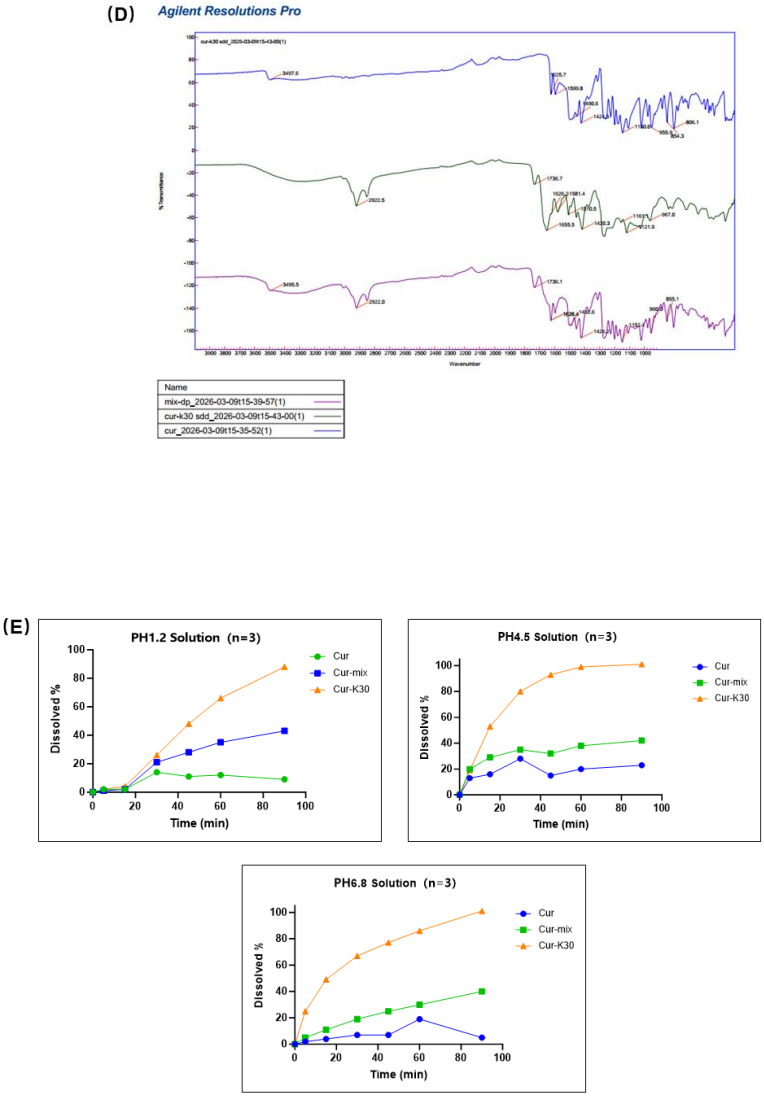


Figure 1. (A) X-ray diffractograms of curcumin, PC, PVP K30, PM, and CSD; (B) DSC of curcumin, PC, PVP K30, PM, and CSD; (C) SEM of curcumin and CSD; (D) FTIR of curcumin, PM, and CSD; (E) In vitro dissolution profiles of curcumin, PM, and CSD in solutions of different pH values (n = 3).

3.2. CSD Attenuates HFD-Induced Hepatic Steatosis

3.2.1. Effects on Body Weight, Liver Weight, and Liver Index

To assess the overall physiological effects of the control condition and the modeling intervention on non-alcoholic fatty liver disease (NAFLD) mice, we firstly measured body weight, absolute liver weight, and liver index (calculated as the ratio of liver weight to body weight). As presented in Figure 2A-E, compared with the control group, the model mice showed a significant increase in final body weight (31.8 ± 0.8 g vs. 29.2 ± 0.8 g, $p < 0.05$). Consistently, absolute liver weight was also significantly higher in the model group (1.26 ± 0.07 g vs. 1.15 ± 0.04 g, $p < 0.01$). However, no significant increase was observed in the liver index. The unchanged liver index, despite the divergent increases in absolute liver weight and body weight, indicates that the hepatic response is systemic and proportional, rather than organ-specific.

© 2026 by the author(s). Distributed under a Creative Commons CC BY license.

Preprints.org | NOT PEER-REVIEWED | Posted: 26 October 2026 https://doi.org/10.20944/preprints202610.2537.v1

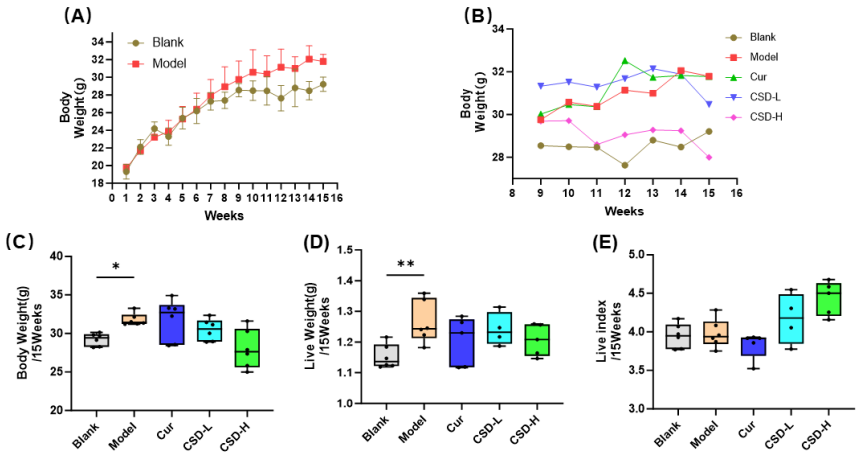


Figure 2. (A) Temporal changes in body weight of the blank control group and model group mice throughout the 15-week modeling period. (B) Temporal changes in body weight of mice in each experimental group from week 9 to week 15 post-treatment. (C) Body weight of mice in each group at the time of euthanasia. (D) Liver weight of mice in each group after euthanasia. (E) Liver index (the ratio of liver weight to body weight) of mice in each group.

3.2.2. Histopathological Evaluation (H&E and Oil Red O Staining)

Hematoxylin-eosin (H&E) staining (Figure 3A) revealed that hepatocytes in the blank control group presented normal morphology, with no observed fatty vacuolation, ballooning degeneration, or inflammatory infiltration. In contrast, the model group displayed diffuse severe hepatic injury, characterized by abundant macrovesicular fatty vacuoles, prominent ballooning degeneration, and focal inflammatory cell infiltration. The curcumin intervention group showed marked histological improvement, with evident reduction in both fatty vacuoles and ballooning degeneration. Low- and high-dose solid dispersion intervention groups exhibited dose-dependent hepatoprotective effects: the low-dose intervention only achieved limited histological amelioration, while the high-dose intervention nearly restored normal hepatocyte morphology, with only occasional tiny lipid droplets observed and no obvious inflammatory infiltration. All treatment groups demonstrated varying degrees of hepatoprotective effects in a dose-dependent manner, and the high-dose solid dispersion group achieved the most prominent histological improvement, with a superior therapeutic outcome compared to the curcumin group.

Oil Red O staining results (Figure 3B) showed that no obvious red lipid droplets were observed in hepatocytes of the blank control group, with a clear background, indicating intact hepatic lipid metabolism. In the model group, diffuse bright-red lipid droplets of varying sizes appeared in hepatocytes, scattered throughout the cytoplasm with deep and dense staining, suggesting significant lipid accumulation. In the curcumin group, the number of red lipid droplets decreased markedly, indicating substantial alleviation of lipid accumulation. The low-dose and high-dose solid dispersion groups showed dose-dependent improvement. The low-dose solid dispersion group exhibited limited amelioration, with a considerable number of red lipid droplets still observed; the high-dose group only displayed occasional tiny lipid droplets, with lipid deposition nearly absent, and the overall effect was superior to that of the curcumin group. Collectively, all treatment groups reduced the area of Oil Red O-positive lipid droplets, and the high-dose solid dispersion group exerted the most prominent inhibitory effect on hepatic lipid accumulation.

© 2026 by the author(s). Distributed under a Creative Commons CC BY license.

Preprints.org | NOT PEER-REVIEWED | Posted: 26 October 2026 https://doi.org/10.20944/preprints202610.2537.v1

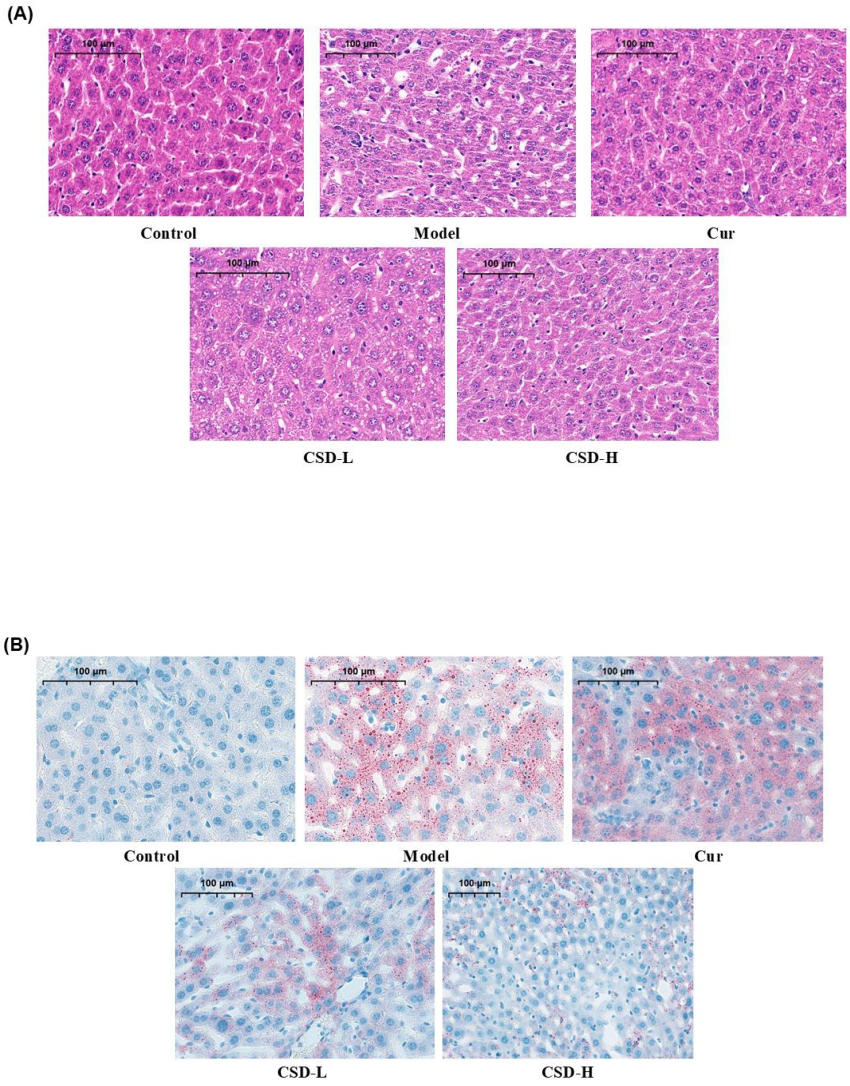


Figure 3. (A) H&E-stained micrographs of liver tissues from each experimental group: (1) normal control group; (2) model group; (3) curcumin group (200 mg·kg^{-1}·d^{-1} p.o) and (4–5) curcumin formulation groups (curcumin-equivalent doses of 50, and 100 mg·kg^{-1}·d^{-1} p.o., respectively). (B) Oil Red O-stained micrographs of liver tissues from each experimental group.

3.3. CSD Improves Serum Biochemical Parameters

3.3.1. Serum Liver Enzyme Levels

Serum alanine aminotransferase (ALT) and alkaline phosphatase (ALP) levels were quantified to assess the hepatoprotective effect of CSD against high-fat diet (HFD)-induced hepatic injury (Figure 4A-B). Compared with the normal control group, the HFD-fed model group showed significantly elevated ALT and ALP levels ($p < 0.001$). Among all experimental groups, the model group exhibited a marked increase in serum ALT relative to the blank control group, confirming the successful establishment of the hepatic injury model. Treatment with curcumin (Cur) significantly reduced ALT levels to a range close to that of the blank control. For CSD intervention groups, the high-dose CSD (CSD-H) group presented the lowest ALT level. These results indicate that both Cur and CSD exert hepatoprotective effects against non-alcoholic hepatic injury, and CSD shows a clear dose-dependent response. For serum ALP, the model group also had significantly higher ALP levels than the blank

© 2026 by the author(s). Distributed under a Creative Commons CC BY license.

Preprints.org | NOT PEER-REVIEWED | Posted: 26 October 2026 https://doi.org/10.20944/preprints202610.2537.v1

control group, which again verified the successful induction of liver injury. Curcumin treatment markedly reduced ALP levels, demonstrating its certain hepatoprotective effect. Furthermore, both low-dose and high-dose CSD groups achieved greater reductions in ALP. The high-dose CSD group had a marginally lower ALP level than the low-dose group, and both groups showed substantially lower ALP levels than the model group. Collectively, CSD exhibits a more potent ALP-lowering effect than curcumin.

3.3.2. Serum Lipid Profile

Serum levels of total cholesterol (TC), low-density lipoprotein cholesterol (LDL-C), and high-density lipoprotein cholesterol (HDL-C) were quantified to assess the effect of CSD on systemic lipid metabolism (Figure 4C–E). Mice in the high-fat diet (HFD)-fed model group developed severe dyslipidemia, characterized by significantly elevated levels of TC, LDL-C, and HDL-C (all $p < 0.0001$, compared with the normal control group). These observations are consistent with well-documented metabolic disturbances induced by high-fat diets. Relative to the model group, intervention with the tested dose of curcumin significantly increased serum HDL-C and TC levels (both $p < 0.001$), while no statistically significant change in LDL-C was detected ($p > 0.05$). In contrast, neither low-dose nor high-dose CSD treatment induced significant differences in HDL-C, LDL-C, or TC levels compared with the model group (all $p > 0.05$). Notably, differences between the two CSD intervention groups were marginal, and no clear dose-dependent trend was observed for any of the three lipid parameters. When comparing the effects of curcumin and CSD, the two interventions exhibited distinct regulatory effects on HDL-C and TC. Overall, these findings indicate that curcumin and its solid dispersions exhibit limited regulatory effects on the serum lipid levels of TC, LDL-C, and HDL-C.

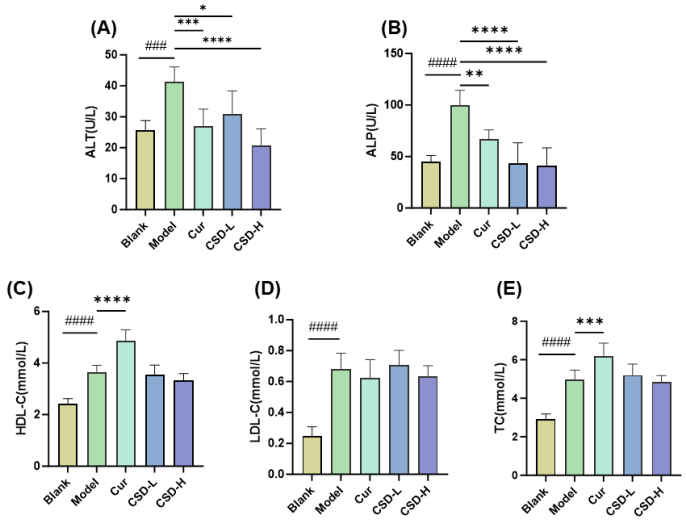


Figure 4. (A) Effects of serum alanine transaminase (ALT), (B) effects of serum alkaline phosphatase (ALP), (C) effects of serum high-density lipoprotein cholesterol (HDL-C), (D) effects of serum low-density lipoprotein cholesterol (LDL-C), (E) effects of serum total cholesterol (TC) in mice fed a high-fat diet (HFD). Data are means ± SD (n = 6 per group). ### and #### represent significance vs. control group, at $p < 0.001$, and $p < 0.0001$, respectively; *, **, *** and ****represent significance vs. model group, at $p < 0.05$, $p < 0.01$, $p < 0.001$, and $p < 0.0001$.

3.3.3. Hepatic Inflammatory Cytokine Levels

To evaluate the anti-inflammatory effects of curcumin and CSD, hepatic levels of pro-inflammatory cytokines (TNF-α, IL-6, and IL-1β) were measured (Figure 5A-C). Compared with the blank control group, all measured inflammatory markers (TNF-α, IL-6, and IL-1β) in the model group were significantly elevated ($P < 0.05$), confirming the successful establishment of the inflammatory model.

© 2026 by the author(s). Distributed under a Creative Commons CC BY license.

Preprints.org | NOT PEER-REVIEWED | Posted: 26 October 2026 https://doi.org/10.20944/preprints202610.2537.v1

In comparison with the model group, the high-dose CSD group exhibited significant reductions in all cytokine levels, with TNF-α and IL-6 approaching those of the blank control group and IL-1β also showing marked improvement. In contrast, the Cur group and the low-dose CSD group only partially decreased TNF-α and IL-1β, but had no significant effect on IL-6. Further intergroup comparisons indicated that the anti-inflammatory efficacy of high-dose CSD was significantly superior to that of Cur and low-dose CSD, and the effect of CSD displayed a clear dose-dependent relationship (high dose significantly more effective than low dose).

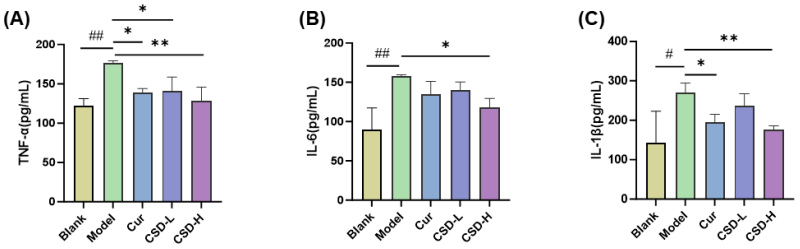


Figure 5. Effects of hepatic levels (A, B, C) of pro-inflammatory cytokines (TNF-α, IL-6, and IL-1β). # and ## represent significance vs. control group, at $p < 0.05$, and $p < 0.01$, respectively; * and **represent significance vs. model group, at $p < 0.05$, $p < 0.01$.

4. Discussion

This study demonstrates that a curcumin solid dispersion (CSD) containing phosphatidylcholine (PC) and polyvinylpyrrolidone K30 (PVP K30) improved in vitro formulation performance and hepatoprotective activity in an experimental model of non-alcoholic fatty liver disease (NAFLD). The disappearance of characteristic curcumin diffraction peaks and its melting endotherm, together with changes in FTIR spectra and particle morphology, is consistent with the formation of an amorphous drug-containing matrix rather than a simple physical blend (Figure 1A–D). This structural change was reflected in apparent solubility values of 184.2, 232.6, and 292.1 μg/mL at pH 1.2, 4.5, and 6.8, respectively, whereas raw curcumin remained below the assay's detection limit (Table 1). After 90 min, CSD released 87.9% of curcumin at pH 1.2 compared with 8.8% from the raw material; release was approximately complete at pH 4.5 and 6.8, compared with 23.5% and 5.4% for raw curcumin (Figure 1E; Tables 2–4). The corresponding physical mixture was less effective, indicating that solid-state modification contributed beyond simple excipient addition. As previous work emphasizes, solubility and membrane permeation are related but not interchangeable properties [23,24]; the animal study therefore provides a valuable complementary test of biological performance.

PC and PVP K30 were combined to integrate phospholipid solubilization with polymer-assisted dispersion and stabilization. PC can associate with hydrophobic compounds and promote their dispersion in aqueous environments, while PVP K30 provides a solid matrix that helps distribute the drug and limits the processing difficulties often encountered with lipid-rich systems. Previous studies reported improved intestinal absorption of mangiferin after phospholipid complexation [25] and enhanced curcumin exposure and hepatoprotective activity with a curcumin–phospholipid complex [26]. However, phospholipid formulations may aggregate or be difficult to solidify, motivating the use of additional carriers [27,28]. Particularly relevant is the report by Zhou et al., in which incorporating a baicalein–phospholipid complex into a PVP K30 matrix increased dissolution and oral bioavailability compared with the phospholipid complex alone [29]. Polymer-containing amorphous dispersions can also offer advantages in solubility and physical stability [30,31]. The broadened FTIR bands are also consistent with noncovalent drug–carrier interactions that could support dispersion

© 2026 by the author(s). Distributed under a Creative Commons CC BY license.

Preprints.org | NOT PEER-REVIEWED | Posted: 26 October 2026 https://doi.org/10.20944/preprints202610.2537.v1

stability. The difference between CSD and the physical mixture supports combining PC and PVP K30 through solvent evaporation, although the individual carrier contributions were not isolated.

These initial benefits also depend on the physical stability of the amorphous matrix. Moisture can plasticize amorphous materials, lower their glass-transition temperature, and increase molecular mobility, thereby facilitating recrystallization [32]. The ability of PVP-based carriers to stabilize amorphous drugs has likewise been shown to depend strongly on relative humidity and storage conditions [33]. Although XRD and DSC indicated that curcumin was amorphous after preparation, these measurements do not establish its long-term stability. Controlled-humidity storage studies with repeated solid-state and dissolution measurements will therefore be important for determining whether performance is maintained throughout storage.

The dissolution behavior can be understood in terms of both amorphization and the maintenance of drug in a dissolved or solubilized state. Because amorphous drug molecules have a higher thermodynamic tendency to dissolve than their crystalline counterparts, they may generate concentrations that exceed crystalline equilibrium solubility. Precipitation or recrystallization can then diminish this advantage [34,35]. PC could assist by associating with the hydrophobic regions of curcumin, whereas PVP K30 could delay nucleation and crystal growth, thereby extending the period during which dissolved drug remains available [36,37]. Supporting studies report improved in vivo performance with PVP-based dispersions [38], increased intestinal drug flux after amorphization [39], and improved curcumin supersaturation with PVP-containing formulations [40]. The higher CSD release across all three media is consistent with these advantages. At the same time, the higher apparent solubility at pH 4.5 and 6.8 than at pH 1.2 demonstrates that the surrounding medium still influences performance. Because the dissolution experiments included sodium dodecyl sulfate and did not directly measure precipitation kinetics or intestinal transport, the specific contributions of supersaturation, micellar solubilization, and permeability cannot yet be separated.

Importantly, the formulation-related improvements observed in vitro were accompanied by meaningful differences in the animal experiments. In the high-fat diet/lipopolysaccharide-induced NAFLD model, high-dose CSD (100 mg/kg/day, expressed as curcumin equivalent) produced the most pronounced histological improvement, with fewer fatty vacuoles, less hepatocellular ballooning, and reduced inflammatory infiltration on H&E staining (Figure 3A). Oil Red O staining similarly showed markedly reduced hepatic lipid deposition, whereas low-dose CSD (50 mg/kg/day) produced more limited changes (Figure 3B). Serum results supported these observations: CSD lowered ALT and ALP, with the lowest ALT in the high-dose group (Figure 4A, B). Inflammatory measurements provided further evidence. High-dose CSD significantly reduced hepatic TNF-α, IL-6, and IL-1β relative to the model group, whereas unformulated curcumin (200 mg/kg/day) and low-dose CSD showed less consistent effects, particularly on IL-6 (Figure 5A–C). Thus, across histopathology, liver injury markers, and hepatic inflammatory responses, CSD at half the curcumin-equivalent dose of unformulated curcumin showed a favorable efficacy pattern. The response was not uniform across all endpoints: neither CSD dose significantly changed serum TC, LDL-C, or HDL-C (Figure 4C–E). Overall, these findings indicate that curcumin and its solid dispersions exhibit limited regulatory effects on the serum lipid levels of TC, LDL-C, and HDL-C.

Previous studies have demonstrated that metabolic dysregulation, inflammatory responses, and innate immune signaling pathways play important roles in the development and progression of non-alcoholic fatty liver disease (NAFLD). C57BL/6J mice were selected because of their susceptibility to high-fat diet (HFD)-induced obesity, metabolic dysfunction, and hepatic steatosis, which resemble several key features of human non-alcoholic fatty liver disease (NAFLD). Although HFD feeding can induce hepatic lipid accumulation and metabolic abnormalities, the extent of hepatic inflammation varies depending on dietary composition and feeding duration. Lipopolysaccharide (LPS), a major component of the outer membrane of Gram-negative bacteria, can promote inflammatory responses through Toll-like receptor 4 (TLR4)-mediated signaling. Therefore, the combination of HFD feeding and LPS administration was employed to investigate hepatic injury and inflammatory responses under conditions of diet-induced metabolic stress. Male mice were used to reduce variability associated

© 2026 by the author(s). Distributed under a Creative Commons CC BY license.

Preprints.org | NOT PEER-REVIEWED | Posted: 26 October 2026 https://doi.org/10.20944/preprints202610.2537.v1

with sex-related differences in metabolic and inflammatory responses, although this limits the generalizability of the findings to females. This experimental model allows the evaluation of the effects of the investigated intervention on body weight, serum biochemical parameters, hepatic histopathology, and inflammatory cytokine levels. Importantly, although the combined HFD and LPS model does not fully reproduce the complex pathogenesis and histopathological spectrum of human NAFLD, it provides a useful experimental approach for investigating the interaction between metabolic dysfunction and endotoxin-associated hepatic inflammation.

The results establish a coherent in vitro–in vivo formulation–performance relationship: conversion of crystalline curcumin into a PC/PVP-based amorphous dispersion was associated with substantially greater apparent solubility and dissolution, followed by improved hepatic outcomes in vivo despite a lower administered curcumin-equivalent dose. This agreement across physicochemical and pharmacodynamic measurements provides strong experimental support for the conclusion that formulation modification enhanced the therapeutic effectiveness of curcumin under the conditions studied, rather than merely improving a laboratory dissolution parameter. Increased dissolution could increase curcumin available for intestinal uptake, aided by phospholipid-mediated solubilization and lipid-associated transport [41,42]. Phospholipids may also influence lymphatic transport [43], although their effects on absorption can depend on formulation composition and are not uniformly beneficial [44]. The present evidence demonstrates enhanced pharmacodynamic performance, but it does not constitute a quantitative in vitro–in vivo correlation or directly establish increased plasma or hepatic exposure. Dose-matched comparisons, pharmacokinetic and tissue-distribution studies, carrier-only and physical-mixture controls, and quantitative histological analysis would help clarify the relative contributions of improved drug delivery and carrier-related effects. Nevertheless, the convergence of dissolution and animal efficacy findings offers a substantive preclinical rationale for further development of this curcumin solid dispersion for NAFLD.

5. Conclusions

In this study, curcumin solid dispersion (CSD) based on PVP K30 and phosphatidylcholine was successfully fabricated via the solvent evaporation method. The ternary formulation converted crystalline curcumin into an amorphous state, markedly improving wettability, equilibrium solubility, and dissolution behavior. The effects, such as the amorphous form of drugs and the formation of supramolecular structures that encapsulate the molecules of active compounds, may be responsible for enhanced solubility. In addition, the increase in solubility is associated with the presence of a phospholipid acting as a solubilizer and stabilizer of the amorphous state.

In a high-fat diet combined with lipopolysaccharide-induced non-alcoholic fatty liver disease (NAFLD) mouse model, oral administration of CSD (50-100 mg/kg for 6 weeks) ameliorated disease phenotypes in a dose-dependent manner, as evidenced by reduced serum alanine transaminase (ALT) and alkaline phosphatase (ALP) levels, attenuated hepatic lipid accumulation, and downregulated pro-inflammatory cytokines (TNF-α, IL-6 and IL-1β). Compared with raw curcumin, CSD showed stronger effects on several measured hepatic injury and inflammatory endpoints. At curcumin-equivalent doses of 50 and 100 mg·kg^{-1}·d^{-1} (p.o.), CSD showed comparable or greater effects than raw curcumin at 200 mg·kg^{-1}·d^{-1} (p.o.) on selected outcomes, suggesting a potential dose-sparing effect under the conditions tested. This pattern may be related to the amorphous form, the hydrophilic PVP K30 matrix, and the solubilizing properties of phosphatidylcholine [44], although direct mechanistic and pharmacokinetic confirmation is needed. A curcumin solid dispersion was developed, and its pharmacodynamic effects were evaluated against NAFLD-related indicators. The integrated evaluation of formulation properties and pharmacodynamic outcomes represents an important contribution of this study. Overall, this work provides preliminary preclinical evidence for curcumin-based solid dispersions as a feasible therapeutic approach for NAFLD.

© 2026 by the author(s). Distributed under a Creative Commons CC BY license.

Preprints.org | NOT PEER-REVIEWED | Posted: 26 October 2026 https://doi.org/10.20944/preprints202610.2537.v1

Author Contributions: Conceptualization, X.G, Y.L, L.S. and Z.G.; methodology, X.G., Q.Z., H.J. and J.Z.; writing—original draft preparation, X.G. and W.Z.; writing—review and editing, X.G., M.L. and C. S.; supervision, C.M and T. L. All authors have read and agreed to the published version of the manuscript.

Funding: This research was funded by the National Natural Science Foundation of China (grant number 82274098) and the National Key Research and Development Program of China (grant number 2023YFC3504200).

Institutional Review Board Statement: The animal study protocol was approved by the Laboratory Animal Ethics Committee of Nanjing University of Chinese Medicine (approval No. A202312050024 on 5 December 2023).

Informed Consent Statement: Not applicable.

Data Availability Statement: The raw data generated and analyzed in this study are available from the corresponding author upon request.

Conflicts of Interest: The authors declare no known competing financial interests or personal relationships that could have influenced the work reported in this paper.

References

1. Stefan, N.; Cusi, K. A global view of the interplay between non-alcoholic fatty liver disease and diabetes. *Lancet Diabetes & Endocrinology* **2022**, *10*, 284-296, doi:10.1016/s2213-8587(22)00003-1.
2. Paik, J.M.; Henry, L.; Younossi, Y.; Ong, J.; Alqahtani, S.; Younossi, Z.M. The burden of nonalcoholic fatty liver disease (NAFLD) is rapidly growing in every region of the world from 1990 to 2019. *Hepatology Communications* **2023**, *7*, doi:10.1097/hc9.0000000000000251.
3. Chattopadhyay, I.; Biswas, K.; Bandyopadhyay, U.; Banerjee, R.K. Turmeric and curcumin: Biological actions and medicinal applications. *Current Science* **2004**, *87*, 44-53.
4. Sanmukhani, J.; Anovadiya, A.; Tripathi, C.B. EVALUATION OF ANTIDEPRESSANT LIKE ACTIVITY OF CURCUMIN AND ITS COMBINATION WITH FLUOXETINE AND IMIPRAMINE: AN ACUTE AND CHRONIC STUDY. *Acta Poloniae Pharmaceutica* **2011**, *68*, 769-775.
5. Salama, A.; Elsherbiny, N.; Hetta, H.F.; Safwat, M.A.; Atif, H.M.; Fathalla, D.; Almanzalawi, W.S.; Almowallad, S.; Soliman, G.M. Curcumin-loaded gold nanoparticles with enhanced antibacterial efficacy and wound healing properties in diabetic rats. *International Journal of Pharmaceutics* **2024**, *666*, doi:10.1016/j.ijpharm.2024.124761.
6. Shahrebabak, M.G.; Haghighi, S.P.S.; Ravankhah, M.; Zare, A.; Bazyari, V.; Izadi, B. A Systematic Review and Meta-analysis of Randomised Controlled Trials on Curcumin-Piperine Supplementation: A Promising Strategy for Managing Lipid Profiles and Liver Health in Non-alcoholic Fatty Liver Disease. *Journal of Herbal Medicine* **2025**, *51*, doi:10.1016/j.hermed.2025.101006.
7. Afarin, R.; Dinarvand, N.; Dariuni, H.A.; Orak, G.; Asl, B.J.; Azizi, R.; Khedri, A. Curcumin and saroglitazar attenuate diet-induced nonalcoholic steatohepatitis by activating the Nrf2 pathway and suppressing ERK1/2 signaling. *Iranian Journal of Basic Medical Sciences* **2024**, *27*, 1015-1022, doi:10.22038/ijbms.2024.75293.16320.
8. Ullah, A.; Hu, S.S.; Shen, B.R. Precision nutrition for NAFLD: a mechanistic rationale for targeting the cytokine landscape. *Frontiers in Cell and Developmental Biology* **2026**, *14*, doi:10.3389/fcell.2026.1745316.
9. Ge, H.J.; Li, J.X.; Xu, Y.; Xie, J.H.; Karim, N.; Yan, F.J.; Mo, J.L.; Chen, W. Curcumin alleviates lipid deposition in hepatocytes through miR-3666/AMPK axis regulation. *Food Bioscience* **2023**, *53*, doi:10.1016/j.fbio.2023.102549.
10. Cheng, M.J.; Ding, F.; Li, L.Y.; Dai, C.M.; Sun, X.L.; Xu, J.; Chen, F.E.; Li, M.X.; Li, X.P. Exploring the role of curcumin in mitigating oxidative stress to alleviate lipid metabolism disorders. *Frontiers in Pharmacology* **2025**, *16*, doi:10.3389/fphar.2025.1517174.
11. Tonnesen, H.H.; Másson, M.; Loftsson, T. Studies of curcumin and curcuminoids. XXVII. Cyclodextrin complexation: solubility, chemical and photochemical stability. *International Journal of Pharmaceutics* **2002**, *244*, 127-135, doi:10.1016/s0378-5173(02)00323-x.

© 2026 by the author(s). Distributed under a Creative Commons CC BY license.

Preprints.org | NOT PEER-REVIEWED | Posted: 26 October 2026 https://doi.org/10.20944/preprints202610.2537.v1

12. Ariaeenejad, S.; Sadeghian-Motahar, S.F. Enhanced solubility, bioaccessibility, and antioxidant activity of curcumin via lipase complexation: Structural insights and stability assessment. *International Journal of Biological Macromolecules* **2025**, *309*, doi:10.1016/j.ijbiomac.2025.142881.
13. Yuan, J.H.; Mao, S.Y.; Ma, X.Z.; Liu, X.L.; Chen, Y.J. Surfactants Significantly Improved the Oral Bioavailability of Curcumin Amorphous Solid Dispersions and Its Underlying Mechanism. *Pharmaceutics* **2025**, *17*, doi:10.3390/pharmaceutics17121541.
14. Seo, S.W.; Han, H.K.; Chun, M.K.; Choi, H.K. Preparation and pharmacokinetic evaluation of curcumin solid dispersion using Solutol® HS15 as a carrier. *International Journal of Pharmaceutics* **2012**, *424*, 18-25, doi:10.1016/j.ijpharm.2011.12.051.
15. Mankan, E.; Sagdic, O.; Karadag, A. Development and Characterization of Spray-Dried Curcumin-Lecithin Complexes with Improved Solubility and In Vitro Digestive and Thermal Stability. *Foods* **2025**, *14*, doi:10.3390/foods14183157.
16. Parikh, A.; Kathawala, K.; Song, Y.M.; Zhou, X.F.; Garg, S. Curcumin-loaded self-nanomicellizing solid dispersion system: part I: development, optimization, characterization, and oral bioavailability. *Drug Delivery and Translational Research* **2018**, *8*, 1389-1405, doi:10.1007/s13346-018-0543-3.
17. Bi, X.L.; Yuan, Z.W.; Qu, B.; Zhou, H.; Liu, Z.Q.; Xie, Y. Piperine enhances the bioavailability of silybin via inhibition of efflux transporters BCRP and MRP2. *Phytomedicine* **2019**, *54*, 98-108, doi:10.1016/j.phymed.2018.09.217.
18. Bondi, A.; Ferrara, F.; Pula, W.; Mariani, P.; Pepe, A.; Drechsler, M.; Montesi, L.; Manfredini, S.; Valacchi, G.; Esposito, E. Spongosome-based co-delivery of curcumin and Piperine: A novel strategy for mitigating pollution-induced skin damage. *Colloid and Interface Science Communications* **2024**, *63*, doi:10.1016/j.colcom.2024.100811.
19. Yu, D.N.; Kan, Z.G.; Shan, F.; Zang, J.; Zhou, J.P. Triple Strategies to Improve Oral Bioavailability by Fabricating Coamorphous Forms of Ursolic Acid with Piperine: Enhancing Water-Solubility, Permeability, and Inhibiting Cytochrome P450 Isozymes. *Molecular Pharmaceutics* **2020**, *17*, 4443-4462, doi:10.1021/acs.molpharmaceut.0c00443.
20. Wdowiak, K.; Miklaszewski, A.; Cielecka-Piontek, J. Amorphous Polymer-Phospholipid Solid Dispersions for the Co-Delivery of Curcumin and Piperine Prepared via Hot-Melt Extrusion. *Pharmaceutics* **2024**, *16*, doi:10.3390/pharmaceutics16080999.
21. Kushwaha, A.K.; Vuddanda, P.R.; Karunanidhi, P.; Singh, S.K.; Singh, S. Development and Evaluation of Solid Lipid Nanoparticles of Raloxifene Hydrochloride for Enhanced Bioavailability. *Biomed Research International* **2013**, *2013*, doi:10.1155/2013/584549.
22. Wdowiak, K.; Pietrzak, R.; Tykarska, E.; Cielecka-Piontek, J. Hot-Melt Extrusion as an Effective Technique for Obtaining an Amorphous System of Curcumin and Piperine with Improved Properties Essential for Their Better Biological Activities. *Molecules* **2023**, *28*, doi:10.3390/molecules28093848.
23. Dahan, A.; Beig, A.; Lindley, D.; Miller, J.M. The solubility-permeability interplay and oral drug formulation design: Two heads are better than one. *Advanced Drug Delivery Reviews* **2016**, *101*, 99-107, doi:10.1016/j.addr.2016.04.018.
24. Beig, A.; Miller, J.M.; Lindley, D.; Carr, R.A.; Zocharski, P.; Agbaria, R.; Dahan, A. Head-To-Head Comparison of Different Solubility-Enabling Formulations of Etoposide and Their Consequent Solubility-Permeability Interplay. *Journal of Pharmaceuti*cal Sciences 2015, 104, 2941-2947, doi:10.1002/jps.24496.
25. Ma, H.Q.; Chen, H.M.; Sun, L.; Tong, L.J.; Zhang, T.H. Improving permeability and oral absorption of mangiferin by phospholipid complexation. Fitoterapia 2014, 93, 54-61, doi:10.1016/j.fitote.2013.10.016.
26. Maiti, K.; Mukherjee, K.; Gantait, A.; Saha, B.P.; Mukherjee, P.K. Curcumin-phospholipid complex: Preparation, therapeutic evaluation and pharmacokinetic study in rats. International Journal of Pharmaceutics 2007, 330, 155-163, doi:10.1016/j.ijpharm.2006.09.025.
27. Jo, K.; Cho, J.M.; Lee, H.; Kim, E.K.; Kim, H.C.; Kim, H.; Lee, J. Enhancement of Aqueous Solubility and Dissolution of Celecoxib through Phosphatidylcholine-Based Dispersion Systems Solidified with Adsorbent Carriers. *Pharmaceutics* **2019**, *11*, doi:10.3390/pharmaceutics11010001.

© 2026 by the author(s). Distributed under a Creative Commons CC BY license.

Preprints.org | NOT PEER-REVIEWED | Posted: 26 October 2026 https://doi.org/10.20944/preprints202610.2537.v1

28. Brinkmann-Trettenes, U.; Barnert, S.; Bauer-Brandl, A. Single step bottom-up process to generate solid phospholipid nano-particles. *Pharmaceutical Development and Technology* **2014**, *19*, 326-332, doi:10.3109/10837450.2013.778875.
29. Zhou, Y.; Dong, W.J.; Ye, J.; Hao, H.Z.; Zhou, J.Z.; Wang, R.Y.; Liu, Y.L. A novel matrix dispersion based on phospholipid complex for improving oral bioavailability of baicalein: preparation, in vitro and in vivo evaluations. *Drug Delivery* **2017**, *24*, 720-728, doi:10.1080/10717544.2017.1311968.
30. Pacult, J.; Rams-Baron, M.; Chmiel, K.; Jurkiewicz, K.; Antosik, A.; Szafraniec, J.; Kurek, M.; Jachowicz, R.; Paluch, M. How can we improve the physical stability of co-amorphous system containing flutamide and bicalutamide? The case of ternary amorphous solid dispersions. *European Journal of Pharmaceutical Sciences* **2019**, *136*, doi:10.1016/j.ejps.2019.06.001.
31. Vullendula, S.K.A.; Nair, A.R.; Yarlagadda, D.L.; Sree, K.S.N.; Bhat, K.; Dengale, S.J. Polymeric solid dispersion Vs co-amorphous technology: A critical comparison. *Journal of Drug Delivery Science and Technology* **2022**, *78*, doi:10.1016/j.jddst.2022.103980.
32. Liu, J.W.; Rades, T.; Grohganz, H. The influence of moisture on the storage stability of co-amorphous systems. *International Journal of Pharmaceutics* **2021**, *605*, doi:10.1016/j.ijpharm.2021.120802.
33. Lehmkemper, K.; Kyerematen, S.O.; Heinzerling, O.; Degenhardt, M.; Sadowski, G. Impact of Polymer Type and Relative Humidity on the Long-Term Physical Stability of Amorphous Solid Dispersions. *Molecular Pharmaceutics* **2017**, *14*, 4374-4386, doi:10.1021/acs.molpharmaceut.7b00492.
34. Schittny, A.; Huwyler, J.; Puchkov, M. Mechanisms of increased bioavailability through amorphous solid dispersions: a review. *Drug Delivery* **2020**, *27*, 110-127, doi:10.1080/10717544.2019.1704940.
35. Pandi, P.; Bulusu, R.; Kommineni, N.; Khan, W.; Singh, M. Amorphous solid dispersions: An update for preparation, characterization, mechanism on bioavailability, stability, regulatory considerations and marketed products. *International Journal of Pharmaceutics* **2020**, *586*, doi:10.1016/j.ijpharm.2020.119560.
36. Baghel, S.; Cathcart, H.; O'Reilly, N.J. Understanding the generation and maintenance of supersaturation during the dissolution of amorphous solid dispersions using modulated DSC and 1H NMR. *International Journal of Pharmaceutics* **2018**, *536*, 414-425, doi:10.1016/j.ijpharm.2017.11.056.
37. Edueng, K.; Mahlin, D.; Larsson, P.; Bergström, C.A.S. Mechanism-based selection of stabilization strategy for amorphous formulations: Insights into crystallization pathways. *Journal of Controlled Release* **2017**, *256*, 193-202, doi:10.1016/j.jconrel.2017.04.015.
38. Knopp, M.M.; Wendelboe, J.; Holm, R.; Rades, T. Effect of amorphous phase separation and crystallization on the in vitro and in vivo performance of an amorphous solid dispersion. *European Journal of Pharmaceutics and Biopharmaceutics* **2018**, *130*, 290-295, doi:10.1016/j.ejpb.2018.07.005.
39. Dahan, A.; Beig, A.; Ioffe-Dahan, V.; Agbaria, R.; Miller, J.M. The Twofold Advantage of the Amorphous Form as an Oral Drug Delivery Practice for Lipophilic Compounds: Increased Apparent Solubility and Drug Flux Through the Intestinal Membrane. *Aaps Journal* **2013**, *15*, 347-353, doi:10.1208/s12248-012-9445-3.
40. Nogami, S.; Minoura, K.; Kiminami, N.; Kitaura, Y.; Uchiyama, H.; Kadota, K.; Tozuka, Y. Stabilizing effect of the cyclodextrins additive to spray-dried particles of curcumin/polyvinylpyrrolidone on the supersaturated state of curcumin. *Advanced Powder Technology* **2021**, *32*, 1750-1756, doi:10.1016/j.apt.2021.03.032.
41. Kuche, K.; Bhargavi, N.; Dora, C.P.; Jain, S. Drug-Phospholipid Complexa Go Through Strategy for Enhanced Oral Bioavailability. *Aaps Pharmscitech* **2019**, *20*, doi:10.1208/s12249-018-1252-4.
42. Fong, S.Y.K.; Brandl, M.; Bauer-Brandl, A. Phospholipid-based solid drug formulations for oral bioavailability enhancement: A meta-analysis. *European Journal of Pharmaceutical Sciences* **2015**, *80*, 89-110, doi:10.1016/j.ejps.2015.08.005.
43. Fricker, G.; Kromp, T.; Wendel, A.; Blume, A.; Zirkel, J.; Rebmann, H.; Setzer, C.; Quinkert, R.O.; Martin, F.; Müller-Goymann, C. Phospholipids and Lipid-Based Formulations in Oral Drug Delivery. *Pharmaceutical Research* **2010**, *27*, 1469-1486, doi:10.1007/s11095-010-0130-x.

© 2026 by the author(s). Distributed under a Creative Commons CC BY license.

Preprints.org | NOT PEER-REVIEWED | Posted: 26 October 2026 https://doi.org/10.20944/preprints202610.2537.v1

44. Jacobsen, A.C.; Ejskjær, L.; Brandl, M.; Holm, R.; Bauer-Brandl, A. Do Phospholipids Boost or Attenuate Drug Absorption? In Vitro and In Vivo Evaluation of Mono- and Diacyl Phospholipid-Based Solid Dispersions of Celecoxib. *Journal of Pharmaceutical Sciences* **2021**, *110*, 198-207, doi:10.1016/j.xphs.2020.08.009.
45. Wdowiak, K.; Tajber, L.; Miklaszewski, A.; Cielecka-Piontek, J. Application of the Box-Behnken Design in the Development of Amorphous PVP K30-Phosphatidylcholine Dispersions for the Co-Delivery of Curcumin and Hesperetin Prepared by Hot-Melt Extrusion. *Pharmaceutics* **2025**, *17*, doi:10.3390/pharmaceutics17010026.

Disclaimer/Publisher's Note: The statements, opinions and data contained in all publications are solely those of the individual author(s) and contributor(s) and not of MDPI and/or the editor(s). MDPI and/or the editor(s) disclaim responsibility for any injury to people or property resulting from any ideas, methods, instructions or products referred to in the content.

© 2026 by the author(s). Distributed under a Creative Commons CC BY license.